

# Automated Method for Extraction of Lung Tumors Using a Machine Learning Classifier with Knowledge of Radiation Oncologists on Data Sets of Planning CT and FDG-PET/CT images\*

Hidetaka Arimura, Ze Jin, Yoshiyuki Shioyama, Katsumasa Nakamura  
Taiki Magome, Masayuki Sasaki

**Abstract**— We have developed an automated method for extraction of lung tumors using a machine learning classifier with knowledge of radiation oncologists on data sets of treatment planning computed tomography (CT) and 18F-fluorodeoxyglucose (FDG)-positron emission tomography (PET)/CT images. First, the PET images were registered with the treatment planning CT images through the diagnostic CT images of PET/CT. Second, six voxel-based features including voxel values and magnitudes of image gradient vectors were derived from each voxel in the planning CT and PET /CT image data sets. Finally, lung tumors were extracted by using a support vector machine (SVM), which learned 6 voxel-based features inside and outside each true tumor region determined by radiation oncologists. The results showed that the average DSCs for 3 and 6 features for three cases were 0.744 and 0.899, and thus the SVM may need 6 features to learn the distinguishable characteristics. The proposed method may be useful for assisting treatment planners in delineation of the tumor region.

## I. INTRODUCTION

Stereotactic radiotherapy (SRT) has been developed for improvement of the clinical outcomes of radiotherapy in the treatment of stable tumors such as brain tumors by delivering very high doses in small irradiation fields. In addition, the stereotactic body radiotherapy (SBRT) has been applied to moving tumors such as lung tumors while immobilizing the body and monitoring tumor locations. In the SBRT technique, the tumor dose could be maximized while the normal tissue dose would be minimized. However, it is assumed that the tumor and organs at risk (OAR) contours should be determined as accurately as possible. The accuracy of contouring or segmentation of tumors affects the precision of radiotherapy, because the prescribed dose distribution in RTP is determined based on the tumor regions, which are manually determined on planning CT images slice-by-slice by a treatment planner. However, the subjective manual contouring is tedious and its reproducibility would be relatively low, resulting in inter-observer variability and

\*Research Grant from Okawa Foundation for Information and Telecommunications, etc.

HA, ZJ, TM, MS are with Department of Health Sciences, Kyushu University, Fukuoka 812-8582, Japan (corresponding author: H. Arimura; e-mail: arimurah@med.kyushu-u.ac.jp).

YS and KN are with Department of Clinical Radiology, Kyushu University, Fukuoka 812-8582, Japan.

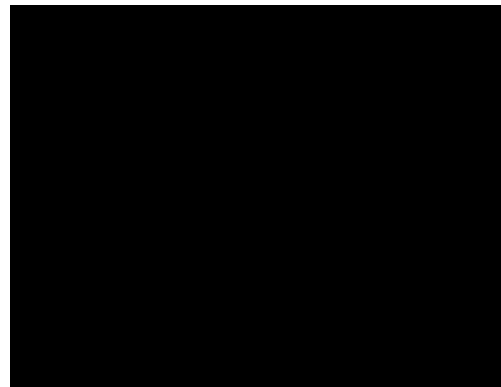


Figure 1. Overall scheme for segmentation of lung tumors using a support vector machine.

intra-observer variability of tumor regions [1-5]. The tumor region is called the gross tumor volume (GTV), which is defined as the visible tumor volume in images. A number of automated contouring methods for the GTVs have been proposed for reducing the inter-observer variability and intra-observer variability, planning time, and increasing the segmentation accuracy of the GTVs. The conventional methods are based on thresholding of the standardized uptake value (SUV) [6,7], a region growing method [5], a Gaussian mixture model [8], a fuzzy c-means algorithm [9], a fuzzy locally adaptive Bayesian approach [10,11], a gradient-based segmentation method [12], a model-based method [13], and an atlas-based method [14]. However, there have been a few studies on segmentation methods for tumor regions based on biological information as well as physical information, such as 18F-fluorodeoxyglucose (FDG)-positron emission tomography (PET) and CT images. In this study, we tried to incorporate the tumor contours determined by radiation oncologists based on the PET biological information and CT morphological information into the proposed contouring method by using a machine learning classifier. Therefore, the aim of this study was to develop an automated method for extracting the GTVs of lung tumors with a support vector machine (SVM), which learned various contours determined by radiation oncologists on planning CT images while taking into account the PET/CT images.

## II. METHODS AND MATERIALS

Figure 1 shows the overall scheme for segmentation of lung tumors using a support vector machine. First, PET

images were registered with the planning CT images through the diagnostic CT images of PET/CT. Second, 6 voxel-based features including voxel values and magnitudes of image gradient vectors were calculated from each voxel in the planning CT and PET/CT image data sets. Third, possible lung GTV voxels were classified by using a support vector machine (SVM), which learned the features inside and outside each true tumor region separately in the training step. Finally, the GTV region was determined by applying morphological closing and opening filters.

#### A. Registration of the PET image to the planning CT image

Prior to the registration, a diagnostic CT image of the PET/CT data set was registered with the PET image using an image position in a Digital Imaging and Communications in Medicine (DICOM) header information and a rigid registration based on normalized mutual information [15]. Figure 2 shows an illustration for registration of a PET image to a planning CT image and a GTV region (radiation therapy structure data) in DICOM-RT (DICOM for radiation therapy). First, the diagnostic CT image of the PET/CT data set was registered with a planning CT image by using an affine transformation matrix. Then, the PET image was registered with the planning CT image and the GTV region by using the same affine transformation matrix, because the PET image was scanned as the same coordinate system as the diagnostic CT image of the PET/CT data set.

#### B. Determination of voxel-based image features

Six voxel-based features were derived for the SVM from each voxel in the planning CT and PET/CT image data sets. All image data, including planning CT images, GTV regions, and PET/CT data sets were placed in the same coordinate system after the registration in the previous step. In general, treatment planners tend to determine GTV contours based on peripheral situations around tumors (e.g. pixel value and gradient) as well as on the tumors themselves. Therefore, each voxel value and its magnitude of image gradient vector were obtained as image features from each voxel in the planning CT image, diagnostic CT and PET images of a PET /CT data set. The image gradient was derived from the following the first-order polynomial within a 5x5x5 voxel region, which was obtained by a least-square method:

$$f(x, y, z) = ax + by + cz + d, \quad (1)$$

where  $x, y,$  and  $z$  are coordinates in a three-dimensional image,  $f(x, y, z)$  is the first-order polynomial, and  $a, b, c,$  and  $d$  are constants. The gradient magnitude  $G$  was defined by the following equation:

$$G = \sqrt{\left(\frac{\partial f}{\partial x}\right)^2 + \left(\frac{\partial f}{\partial y}\right)^2 + \left(\frac{\partial f}{\partial z}\right)^2} = \sqrt{a^2 + b^2 + c^2}. \quad (2)$$

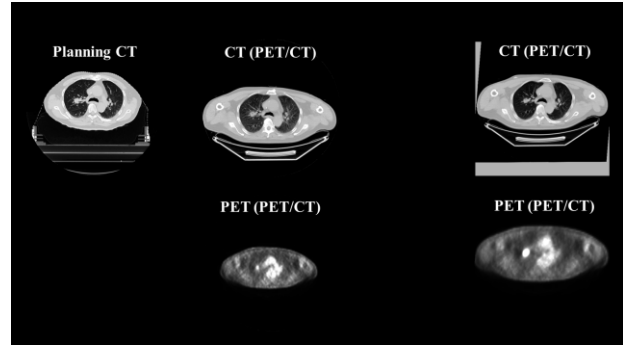


Figure 2. An illustration for registration of a PET image to a planning CT image and a GTV region.  $T_{affine}$  is an affine transformation matrix.

#### C. Segmentation of the GTV region using a support vector machine

SVM is one of machine learning classifiers, which is believed to have high generalization ability, avoidance of local minimum traps, and ability to overcome the curse of dimensionality. In the training stage of the SVM, a mathematical model representing the relationship between input data (voxel-based image features) and teaching data (+1: inside GTV, -1: outside GTV) can be constructed by changing weighting factors in the mathematical model.

Our basic idea of this study was to feed tumor contours determined based on radiation oncologists' knowledge and experience into a machine learning system in a training step, which can classify objective voxels in a region of interest (ROI) into the "possible voxels" of GTV and normal tissue in testing step. The GTVs were extracted by using a support vector machine, which learned 3 or 6 voxel-based features inside and outside each true tumor region (ground truth). The teacher signal was plus one if the voxel was inside the GTV region, whereas the teacher signal was minus one if the voxel was outside the GTV. The outside region of the GTV was defined as the region dilated six times by a circle kernel with a radius of 1 mm. The training voxels were selected at various sampling intervals depending on the ratio between the numbers of inside and outside voxels, so that the number of the inside voxels could be the same as that of outside voxels. We constructed an SVM classifier with a Gaussian kernel, i.e.,  $\exp(-\gamma\|x - y\|^2)$ , by using the open source software package SVM light [16]. In this study, the value  $\gamma$ , the parameter C, and the threshold value were set as 0.0001, 12.5, and 0.50, respectively. Finally, the GTV region was determined by successively applying mathematical morphological closing and opening filters.

#### D. Clinical test cases

Data sets of planning computed tomography (CT) and positron emission tomography (PET)/CT images of three lung cancer patients, who received SBRT, were selected for this study. All patients were scanned by using a 4-slice CT scanner (Mx 8000; Philips, Eindhoven, NL) to acquire planning CT images with a pixel size of 0.977 mm in axial

plane and a slice thickness of 2.0 mm. Planning CT images were employed for segmentation of the tumor region and calculation of dose distribution in patient body in the RTP system, whereas PET/CT image sets were obtained for assisting the treatment planner in delineation of the tumor region. The CTVs were determined based on a consensus between two experienced radiation oncologists on the planning CT images with considering PET/CT images using a radiation treatment planning system (Eclipse version 6.5 and 8.1; Varian Medical Systems Inc., Palo Alto, CA). The mean effective diameter of GTV was 22.4 mm with 18.9 - 25.7 mm. The PET/CT data sets were acquired during shallow free breathing on a PET/CT scanner (GE, Discovery STE) with a 16-slice CT scanner. The PET images were obtained with 3 min per bed position and 60 min after injection of a certain dose (mean dose: 222.5 MBq) of 18F-FDG. The PET images were scatter and attenuation corrected, and they were reconstructed by use of three-dimensional ordered-subset expectation maximization with a post reconstruction Gaussian filter of 6 mm in the full width at half maximum, 28 subsets, and 2 iterations. In data sets of PET/CT, the matrix size, pixel sizes in plane, and slice thicknesses are 512 x 512, 0.977 mm, and 5 mm for CT images, and 128 x 128, 5.47 mm and 3.27 mm for PET images, respectively. Each image data set and GTV data were converted into the isotropic images with a voxel size of 0.977 mm by using a cubic interpolation for planning CT and diagnostic CT images of a PET/CT scatter, PET images for a tri-linear interpolation method, and a shape-based interpolation method [17] for GTV.

### E. Evaluation of proposed method

We performed the leave-one-out-by-patient test for the SVM-based segmentation method using 57 slices. In the validation test, we calculated the Dice similarity coefficient (DSC), which indicates the degree of coincidence between GTV regions determined by the manual method and the proposed method. The DSC  $S$  is defined as

$$S = \frac{2n(T \cap C)}{n(T) + n(C)}, \quad (3)$$

where  $T$  is the “ground truth” region, manually determined by two radiation oncologists,  $C$  is the GTV region obtained by using the proposed method,  $n(T \cap C)$  is the number of logical AND pixels between  $T$  and  $C$ ,  $n(T)$  is the number of voxels in the ground truth region and  $n(C)$  is the number of voxels in the GTV region.

## III. RESULTS AND DISCUSSION

The GTVs extracted by using the support vector machine, which learned 3 or 6 voxel-based features inside and outside each true tumor region, are shown in Figure 3 with the DSC between the gold standard and regions segmented by the proposed method. The three features were the voxel values of the planning CT image and diagnostic CT, and the SUV of PET images. Estimated GTV regions are shown in green, and the borders of the GTV contoured by radiation oncologists are indicated with red lines. In addition, overlap lines between the GTV outline and the estimated GTV are shown in yellow. The results showed that the average DSCs for 3 and 6 features

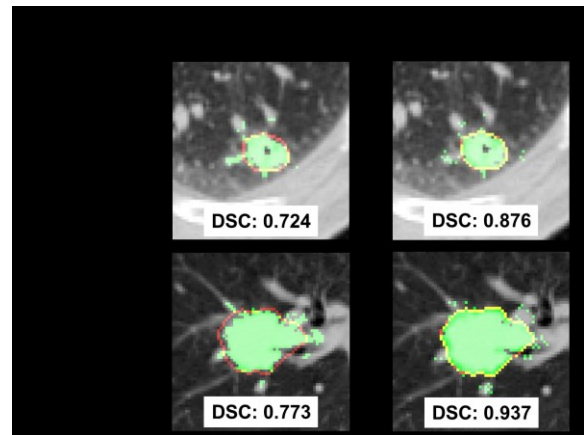


Figure 3. GTVs extracted by using the support vector machine, which learned 3 or 6 voxel-based features inside and outside each true tumor region.

were 0.744 and 0.899, and thus the SVM may need 6 features to learn the distinguishable characteristics. In addition, it might be a little more difficult for the SVM to learn the mixed grad glass opacity (GGO) tumor compared with the solid tumors.

El Naqa *et al* [18] developed a multimodality segmentation method using a multivalued level set method, which can provide a feasible and accurate framework for combining imaging data from different modalities (PET/CT), and is a potentially useful tool for the delineation of biophysical structure volumes in radiotherapy treatment planning. On the other hand, in this study, we tried to incorporate the tumor contours determined by radiation oncologists based on the PET biological information and CT morphological information into the proposed contouring method by using a machine learning method.

### ACKNOWLEDGMENT

The authors are grateful to all members of Arimura laboratory (<http://www.shs.kyushu-u.ac.jp/~arimura>) for valuable comments and helpful discussion. This research was partially supported by the Ministry of Education, Culture, Sports Science, and Technology (MEXT), Grant-in-Aid for Scientific Research (C), 22611011, 2011 to 2012, and Grant-in-Aid for Scientific Research on Innovative Areas, 24103707, 2012.

### REFERENCES

- [1] International Commission on Radiation Units & Measurements (ICRU), *ICRU report 62, Prescribing, Recording and Reporting Photon Beam Therapy*. (Supplement to ICRU Report 50), 1999.
- [2] J. Van de Steene, N. Linthout, J. de Mey, V. Vinh-Hung, C. Claassens, M. Noppen, A. Bel, G. Storme, “Definition of gross tumor volume in lung cancer: inter-observer variability,” *Radiotherapy and Oncology* vol.62, pp. 37-49, Jan. 2002
- [3] J.D. Bradley, C.A. Perez, F. Dehdashti, B.A. Siegel, “Implementing biologic target volumes in radiation treatment planning for non-small

- cell lung cancer," *Journal of Nuclear Medicine* vol. 45, pp 96S-101S, Jan. 2004.
- [4] K. Nakamura, Y. Shioyama, S. Tokumaru, N. Hayashi, N. Oya, Y. Hiraki, K. Kusuohara, T. Toita, H. Suefuji, N. Hayabuchi, H. Terashima, M. Makino, K. Jingu, "Variation of clinical target volume definition among Japanese radiation oncologist in external beam radiotherapy for prostate cancer," *Jpn J. Clin. Oncol.*, vol.38 no.4, pp. 275-280, Apr. 2008.
- [5] E. Day, J. Betler, D. Parda, B. Reitz, A. Kirichenko, S. Mohammadi, M. Miftten, "A region growing method for tumor volume segmentation on PET images for rectal and anal cancer patients," *Med. Phys.*, vol. 36, no.10, pp.4349-4358, Oct. 2009.
- [6] K.J. Biehl, F.M. Kong, F. Dehdashti, J.Y. Jin, S. Mutic, I. El Naqa, B.A. Siegel, J.D. Bradley, "18F-FDG PET definition of gross tumor volume for radiotherapy of non-small cell lung cancer: Is a single standardized uptake value threshold approach appropriate?" *Journal of Nuclear Medicine*, vol.47, no.11, pp. 1808-1812, Nov. 2006.
- [7] T. Zhang, Y. Tachiya, Y. Sakaguchi, K. Mitsumoto, T. Mitsumoto, N. Ohya, M. Sasaki, "Phantom study on three-dimensional target volume delineation by PET/CT-based auto-contouring," *Fukuoka Acta Media* vol.101, no.11, pp. 238-246, Nov. 2010.
- [8] M. Aristophanous, B.C. Penney, M.K. Martel, C.A. Pelizzari, "Gaussian mixture model for definition of lung tumor volumes in positron emission tomography," *Med. Phys.*, vol. 34, no.11, pp. 4223-4235, Nov. 2007.
- [9] S. Belhassen, H. Zaidi, "A novel fuzzy C-means algorithm for unsupervised heterogeneous tumor quantification in PET," *Med. Phys.*, vol. 37, no.3, pp. 1309-1324, Mar. 2010.
- [10] M. Hatt, C. Cheze le Rest, A. Turzo, C. Roux, D. Visvikis. "A fuzzy locally adaptive Bayesian segmentation approach for volume determination in PET," *IEEE Transactions on Medical Imaging*, vol. 28, no.6, pp. 881-893, Jun. 2009.
- [11] M. Hatt, C. Cheze Le Rest, N. Albarghach, O. Pradier, D. Visvikis, "PET functional volume delineation: a robustness and repeatability study," *European Journal of Nuclear Medicine and Molecular Imaging*, vol. 38, pp. 3663-3672, Apr.2011.
- [12] X. Geets, JA. Lee, A. Bol, M. Lonneux, V. Gregoire. "A gradient-based method for segmenting FDG-PET images: methodology and validation," *European Journal of Nuclear Medicine and Molecular Imaging*, vol. 34, pp. 1427-1438, Sep.2007.
- [13] Mikael Rousson, Ali Khamene, Mamadou Diallo, Juan Carlos Celi, Frank Sauer. "Constrained surface evolutions for prostate and bladder segmentation in CT images," Lecture notes in computer science (LNCS), edited by Liu Y, Jiang T, and Zhang C, New York: Springer, 2005, vol.3765, pp. 251-260.
- [14] G. Strassmann, S. Abdellaoui, D. Richter, F. Bekkaoui, M. Haderlein, E. Fokas, N. Timmesfeld, B. Vogel, M. Henzel, R. Engenhardt-Cabillic, "Atlas-based semiautomatic target volume definition (CTV) for head-and-neck tumors," *Int. J. of Radiat. Oncol. Biol. Phys.*, vol. 78, no.4, pp. 1270-1276, Nov.2010.
- [15] J.P. Pluim, J.B. Maintz, M.A. Viergever, "Mutual-information-based registration of medical images: a survey," *IEEE Trans. Med. Imaging*, vol. 22, no.8, pp. 986-1004, Aug. 2003.
- [16] T. Joachims, SVMlight. Cornell University, 2008.  
<http://svmlight.joachims.org/>
- [17] G.T. Herman, J. Zheng, C.A. Bucholtz, "Shape-based interpolation," *IEEE Comput. Graph. Appl.*, vol.12, pp. 69-79, 1992.
- [18] I. El Naqa, D. Yang, A. Apte, D. Khullar, S. Mutic, J. Zheng, J.D. Bradley, P. Grigsby, J.O. Deasy, "Concurrent multimodality image segmentation by active contours for radiotherapy treatment planning," *Med. Phys.*, vol.34, no.2, pp. 4738-4749, Dec. 2007.